Magneto-Motive Force and Performance Comparative Analysis Research for a Novel Pentacle-Star Hybrid Winding Five-Phase Induction Motor

Jinhong Li and Dawei Meng*

Abstract—In order to shorten design optimization cycle and reduce the influence of low-order harmonic for multi-phase induction motor, two kinds of five-phase motors — using either a star or pentacle-star hybrid winding — are proposed based on Y160L-4 three-phase induction motor, which keep the structure size of the stator and rotor and rated power constant, redesign the winding, and adjust the match parameters of the stator and rotor slots. Based on the Fourier series expansion method, the time-space harmonic Magneto-Motive Force (MMF) analytic function of pentacle-star winding was given based on star winding MMF. According to the analysis for the MMF table of three kinds of induction motors, pentacle-star winding with 19th-order harmonic has a better performance than star-winding with 9th-order harmonic and three-phase delta winding with 5th-order harmonic. Further analysis suggests that the harmonic torque generated by the harmonic MMF can be used to improve the electromagnetic torque, and the effective torque characteristics of the three forms of induction motors are given. Two kinds of five-phase motors with different winding configurations can be realized based on the three-phase motor, and some simulated and experimental results show that the method is feasible, which provides significant value in engineering applications.

1. INTRODUCTION

Due to several advantages, such as lower voltage with high power, lower torque ripple, higher fault-tolerance capability, lower DC link current harmonics, and high reliability and efficiency, compared with conventional three-phase motors, multi-phase motors have been used in many fields, including electric locomotives, electric ship propulsion systems, aerospace engineering, wind power, and hybrid-electric vehicles [1–6]. A five-phase motor is a typical representative multi-phase motor, which was first proposed in 1969 with inverter-fed voltage source [7].

In high-power fault-tolerant electric drive systems, multiphase machines have been found to be favorable, due to the various merits offered by such machines [8]. A multi-phase motor can be fed from either a five-phase generator or a voltage/current source inverter, but its space vector is greatly increased, due to the increase of the number of stator phases in the motor. Further, the voltage or current waveform output by the inverter is not a standard sine wave, but contains a harmonic component which cannot be ignored, and the produced harmonic Magneto-Motive Force (MMF) has a great influence on the operational performance of the motor. Therefore, many research institutes and universities have paid attention to the following four aspects: 1) the structural design of multi-phase motors, as good structural design can effectively reduce the influence of spatial harmonics on motor performance (e.g., start-up performance and magnetic noise); 2) the relationship between harmonic current and the

harmonic MMF of multi-phase motors with different structure under a non-sinusoidal power supply; 3) how to effectively use the harmonics to improve motor performance; and 4) fault diagnosis and fault-tolerant control of multi-phase motors [1–14].

Magnetic Finite Element Analysis (FEA) and algebraic equation analysis based on the permeance model have been used to analyze the harmonic components of air-gap flux density distribution when designing induction motors [9, 10]. Time and spatial harmonics have been researched using analytical methods and equivalent circuit methods [11, 12]. Using four stator winding modes combined by even or odd number phase, symmetric or semi-symmetric winding construction can be analyzed [13]. In order to reduce the spatial harmonic content of the MMF, a new technique to design a squirrel cage induction motor has been proposed in a three-phase motor [14]. A star winding five-phase variable-speed driven motor has been researched [15]. A combined star-delta winding three-phase induction motor has been analyzed to resolve the low spatial harmonic [16, 17]. The effects of three stator winding configurations for a five-phase motor have been studied [18]. The phase transposition effect with different stator winding connections in a five-phase motor has been studied [19]. A fault-tolerant and steady-state model has been studied in depth for a combined star-pentagon stator winding connection five-phase motor [20, 21]. A generalized optimal fault-tolerant control strategy for different winding connections of a five-phase motor has been proposed [22]. In order to effectively use the existing three-phase motor structure and reduce the design cost as much as possible, we study the possibility of transforming the traditional three-phase motor into a multi-phase motor in this paper. A Space Vector analysis method, slot number phase diagram method and complex analytic method [23] are used to analyze multi-phase motor harmonic MMF.

The remainder of the paper is organized as follows: Section 2 introduces the realization of two types of winding configurations for a five-phase motor based on the Y160L-4 three-phase motor. Section 3 illustrates the MMF of star winding connection and pentacle-star connection in the five-phase motor, and the MMF and electromagnetic torque characteristics for three kinds of motors are analyzed and compared. Section 4 shows the results of the simulation analysis and the experiment of two kinds of five-phase motor. The discussion and conclusion sections follow.

2. TWO TYPES OF WINDING CONFIGURATION FOR A FIVE-PHASE MOTOR

2.1. Two Kinds of Winding Configuration

In order to decrease design and manufacturing costs and maximize the use of existing motor structure parameters, such as those of the Y160L-4, an idea which transforms a three-phase motor into a multi-phase motor is proposed. For a multiphase machine with an odd number of phases n, there are $(n+1)/2$ connection alternatives [24–26]. For example, a five-phase stator winding has three types of winding
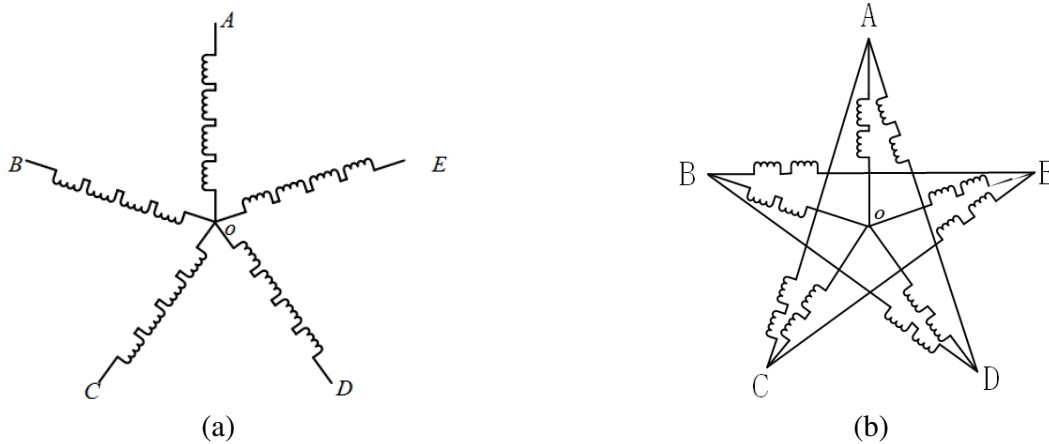

Figure 1. Star and novel pentacle-star winding configuration for a five-phase motor. (a) Star winding. (b) Pentacle-star winding.

configurations, namely, star, pentagon, and pentacle. One kind of the winding researched in this paper is that in Figure 1(a), where the phase shift is 72° between adjacent phases. One end of the winding is the winding overhang (phases A-E), while the other end of winding is connected to all others (the common point O). Y160L-4 is the most mature three-phase induction motor of China, where Y stands for the production model; 160 is the central height of the motor from axis to the ground (unit: mm); L stands for long iron core; and 4 stands for the pole number.

Increasing the number of phases can also provide an effective means to increase the order of the lowest-order harmonics; the corresponding induced rotor currents due to these flux harmonic components will be less significant. The novel pentacle-star winding configuration shown in Figure 1(b) was proposed by rewiring windings. Every phase winding was divided into two winding groups; for example, phase A winding was divided into winding $A1$ and winding $A2$. Winding $A1$ keeps the star configuration, and winding $A2$ is shifted in space by one slot (or 18° electrical degrees), thus forming a pentacle configuration.

2.2. Winding Diagram and Main Performance Parameters

Taking the Y160L-4 three-phase induction motor with 15 kW as a benchmark, with the rated power and the size of the three circles unchanged, two types of five-phase induction motors (with star winding configuration and pentacle-star winding configuration) were designed, in which the connection method of the stator winding, the number of conductors of the stator/rotor, and the slot diagram of the stator/rotor are redesigned.

Figure 2 and Figure 3 show the wiring expansion diagram of two types of five-phase motor, namely conventional star winding five-phase motor and novel pentacle-star winding five-phase motor. Table 1 shows the parameters difference of three types of motors. The other materials and dimensions are the same as the Y160L-4 three-phase induction motor.
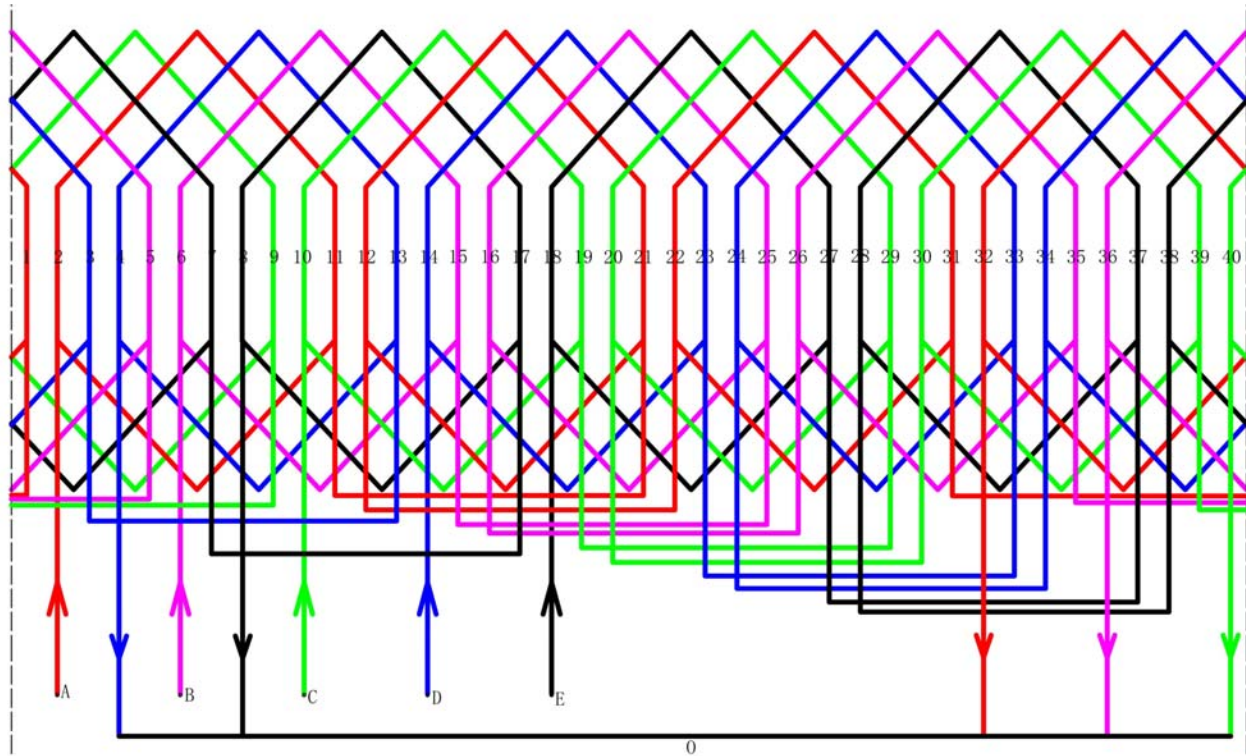
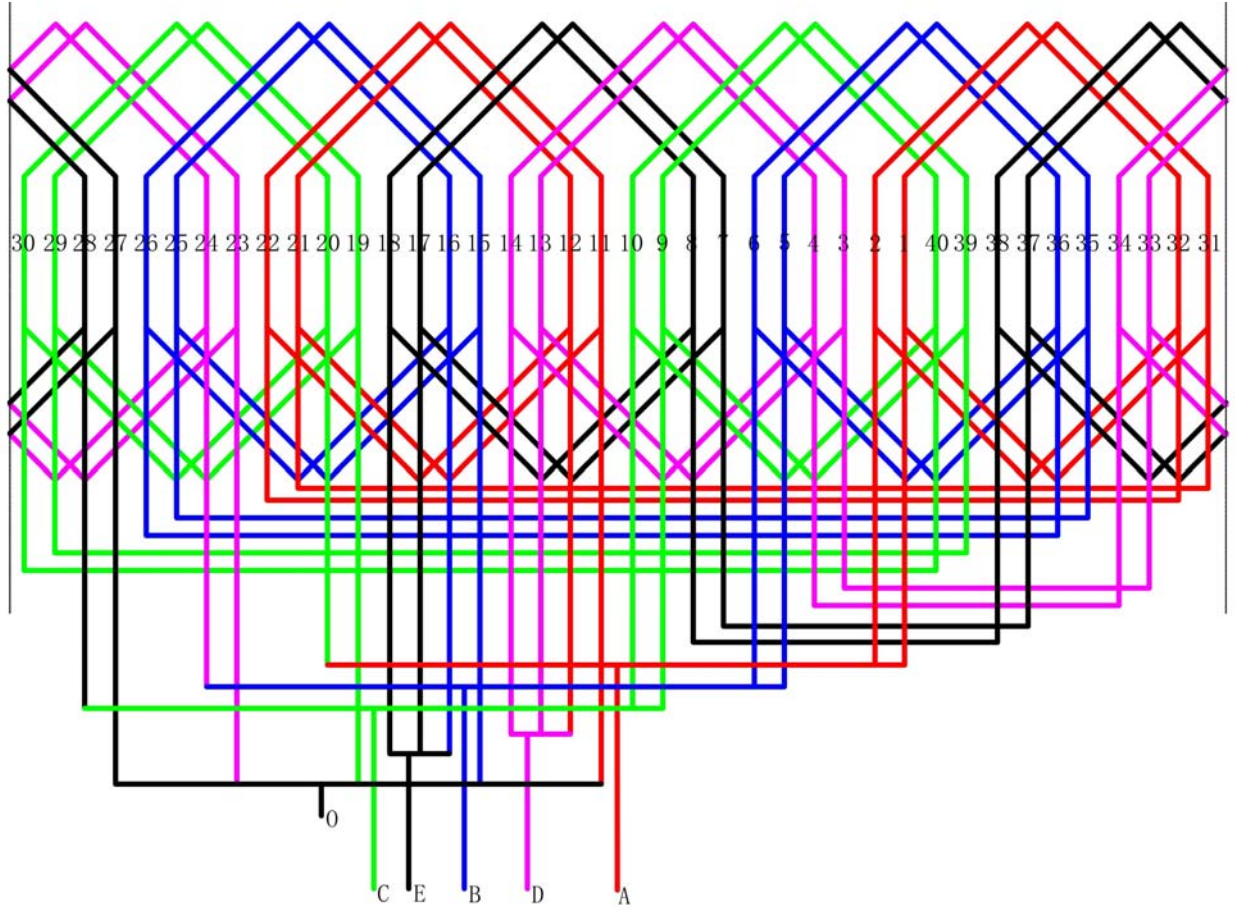

Figure 2. Star winding diagram.

Figure 3. Pentacle-star winding diagram.

3. TWO TYPES OF FIVE-PHASE WINDING MMF ANALYSIS

3.1. Star Winding MMF Analysis

In order to analyze the MMF of the pentacle-star winding, time and spatial coordinate systems were given, based on the star winding with concentrated and full-pitch windings and 72° (electrical degrees) between adjacent phases. Figure 4 shows the spatial coordinate system with 40/34, which takes the axis of the phase A winding as the ordinate, indicating the magnitude of MMF, while the abscissa is placed on the inner surface of the stator. Counterclockwise is considered the positive direction. α indicates the included angle between any position on the circumference of the air gap and the axis of the phase A winding (in the counterclockwise direction). The time coordinate system takes the effective value of the current as the ordinate, indicating the magnitude of the phase current, and the time t as the abscissa, where the starting time moment is the maximum value moment when the fundamental current flows through the phase A winding.

MMF is the function of time and space. When spatial coordinate system is given, for concentrated full-pitch winding, according to Figure 5, the winding function can be expressed as in

$$N_A(\alpha) = \begin{cases} \dfrac{1}{2}N, & 0 \leq \alpha \leq \pi \\ -\dfrac{1}{2}N, & \pi \leq \alpha \leq 2\pi \end{cases} \tag{1}$$

where N is the number of turns per coil for phase A.

Table 1. Different parameters of three types of induction motor.

| Phase number	3	5	5
Winding configuration	Delta connection	Star connection	Pentacle-star connection
Slot fit	36/26	40/34	40/34
Winding overhang	3	5	5
Core length	195 mm	190 mm	190 mm
Number of conductors in one slot	22	18	18 (star)/34 (pentacle)
Wire gauge	2–2.15 mm, 1–1.18 mm	2–1.06 mm, 2–1.0 mm	2–1.06 mm, 2–1.0 mm (star), 3–0.85 (pentacle)
Line voltage	380 V	253 V	203 V
Rotor skewed length	11.1 mm (all slots)	0	0
Full ratio of stator slot	77.8%	77%	77% (star), 76.8% (pentacle)
Line current	29.67 A	18.19 A	27.86 A
Torque	97.95 Nm	98.03 Nm	98.08 Nm
Efficiency	0.8975	0.904	0.908
Power factor	0.8561	0.8516	0.8622
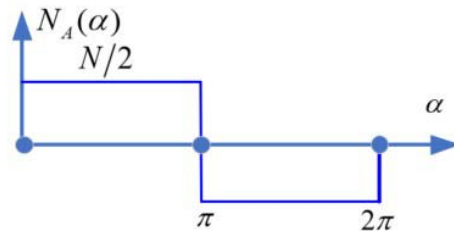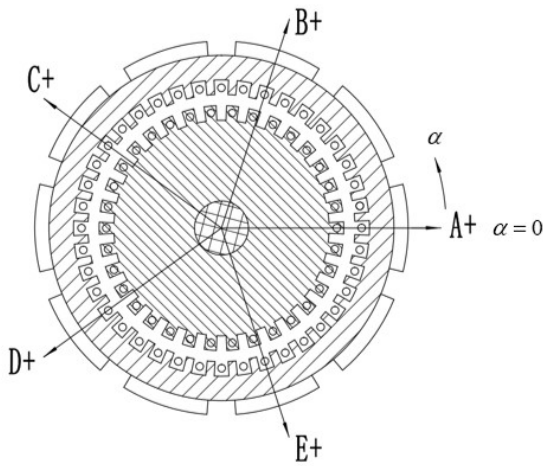
Figure 4. Star winding co-ordinate system diagram.

Figure 5. Winding function of phase A for star winding.

According to Equation (1), the Fourier series of the winding function of phase A can be expressed as in

$$N_A(\alpha) = \sum_{v=1,3,5...}^{\infty} N_v \cos(v\alpha) \tag{2}$$

where N_v is the amplitude of v-order harmonic turns, $N_v = 2N \sin(v\pi/2)/(v\pi)$, $v = 1, 3, 5...$

In the same way, the current of the winding of phase A can be expressed as in

$$I_A(t) = \sum_{u=1,3,5...}^{\infty} \sqrt{2} I_u \cos(u\omega t)) \tag{3}$$

where I_u is the effective of the u-order harmonic current.

The Fourier series is used to give the winding function, expressing the frequency of the spatial harmonic windings and obtain the u order harmonic current expression, when adopting a non-sinusoidal power supply. According to the winding function theory of AC motors, the u-order harmonic currents of every phase winding generated by v-order harmonic MMF can be given as [27, 28]

$$
\begin{cases}
f_{A(u-v)}(\alpha, t) = \sqrt{2} N_v I_u \cos(v\alpha) \cos(u\omega t) \\[2mm]
f_{B(u-v)}(\alpha, t) = \sqrt{2} N_v I_u \cos\left(v\left(\alpha - \frac{2\pi}{5}\right)\right) \cos\left(u\left(\omega t - \frac{2\pi}{5}\right)\right) \\[2mm]
f_{C(u-v)}(\alpha, t) = \sqrt{2} N_v I_u \cos\left(v\left(\alpha - \frac{4\pi}{5}\right)\right) \cos\left(u\left(\omega t - \frac{4\pi}{5}\right)\right) \\[2mm]
f_{D(u-v)}(\alpha, t) = \sqrt{2} N_v I_u \cos\left(v\left(\alpha - \frac{6\pi}{5}\right)\right) \cos\left(u\left(\omega t - \frac{6\pi}{5}\right)\right) \\[2mm]
f_{E(u-v)}(\alpha, t) = \sqrt{2} N_v I_u \cos\left(v\left(\alpha - \frac{8\pi}{5}\right)\right) \cos\left(u\left(\omega t - \frac{8\pi}{5}\right)\right)
\end{cases} \tag{4}
$$

By using the trigonometric transformation formula from integration to difference, Formula (4) can be converted to

$$
f_{*(u-v)}(\alpha, t) = \frac{\sqrt{2}}{2} N_v I_u \left(\cos\left(v\alpha - u\left(\omega t - \frac{2\pi}{5}n\right)\right) + \cos\left(v\alpha + u\left(\omega t - \frac{2\pi}{5}n\right)\right)\right) \tag{5}
$$

where $n = 0, 1, 2, 3, 4$, and $*$ indicates A, B, C, D, or E.

According to Formula (5), each phase harmonic MMF can be decomposed into two rotating MMFs with the same amplitude, same speed, and opposite directions, which are called forward rotating MMF and reverse rotating MMF.

The total MMF of the star winding can be obtained by using the superposition principle, as shown in Formula (6)

$$
f_{(u-v)}(\alpha, t) = \begin{cases}
5\frac{\sqrt{2}}{2} N_v I_u \cos(v\alpha + u\omega t), & u + v = 10k, \ k = 0, \pm 1, \pm 2 \\[2mm]
0, & u \pm v \neq 10k, \ k = 0, \pm 1, \pm 2 \\[2mm]
5\frac{\sqrt{2}}{2} N_v I_u \cos(v\alpha - u\omega t), & u - v = 10k, \ k = 0, \pm 1, \pm 2
\end{cases} \tag{6}
$$

When $u = 1$ and $v = 3, 5, 7$, the total MMF generated by fundamental current is zero. When $u = 1$ and $v = 9, 11$, the total MMF generated by fundamental current is expressed as

$$
\begin{cases}
f_{(1-9)}(\alpha, t) = 5\frac{\sqrt{2}}{2} N_v I_u \cos(9\alpha + \omega t) \\[2mm]
f_{(1-11)}(\alpha, t) = 5\frac{\sqrt{2}}{2} N_v I_u \cos(11\alpha - \omega t)
\end{cases} \tag{7}
$$

As the moving direction and speed of any point on the MMF are the same, the largest amplitude point is selected to calculate the angular velocity of the MMF, which satisfies

$$
\begin{cases}
9\alpha + \omega t = 0 \\
11\alpha - \omega t = 0
\end{cases} \tag{8}
$$

The angular velocity of harmonic motion can be obtained. Furthermore, the angular velocity of the u-order harmonic MMF generated by the v-order harmonic current of the star winding can be obtained by adopting the above method, as shown

$$
\omega_v = \begin{cases}
-\dfrac{v\omega}{u}, & u + v = 10k, \ k = 0, \pm 1, \pm 2 \\[2mm]
0, & u + v \neq 10k, \ k = 0, \pm 1, \pm 2 \\[2mm]
+\dfrac{v\omega}{u}, & u - v = 10k, \ k = 0, \pm 1, \pm 2
\end{cases} \tag{9}
$$

where "+" indicates the forward rotating MMF, and "−" indicates the reverse rotating MMF.

3.2. Pentacle-Star Winding MMF Analysis

The pentacle-star winding is composed of two sets of five-phase single-layer concentrated windings. The first winding ($A1$ set) is connected in star configuration, while the second winding ($A2$ set) is connected in pentacle; together, they produce the harmonic MMF. The winding can be considered as an asymmetrical ten-phase winding or a split-phase dual five-phase winding. This section mainly gives the expression of the MMF formed by the fundamental current and subspace harmonic.

The phase voltages and current of the star and pentacle windings satisfy the following relationship [29, 30]

$$V_{A2} = 1.902 V_{A1} \tag{10}$$
$$I_{A1} = 1.902 I_{A2} \tag{11}$$

where V_{A2} and V_{A1} respectively represent the phase voltage of the pentacle and star winding.

Hence, to obtain the same MMF magnitude from the two winding sets, for equal ampere turn for both windings $N_{C1}I_{A1} = N_{C2}I_{A2}$. The relation between the number of turns per phase for the two winding sets is expressed as

$$N_{C2} = 1.902 N_{C1} \tag{12}$$

where N_{C1} is the number of turns of star winding $A1$, and N_{C2} is the number of turns of the pentacle winding $A2$. This gives the same copper volume as in a conventional five-phase winding. The Fourier series of the winding functions of the windings $A1$ and $A2$ can be expressed as

$$\begin{cases} N_{A1}(\alpha) = \sum_{v=1,3,5...}^{\infty} \dfrac{2N_{C1}}{v\pi} \cos(v\alpha) \\[4mm] N_{A2}(\alpha) = \sum_{v=1,3,5...}^{\infty} \dfrac{2N_{C2}}{v\pi} \cos\left(v\left(\alpha - \dfrac{\pi}{10}\right)\right) \end{cases} \tag{13}$$

Further, the v-order harmonic MMF generated by fundamental current can be expressed as

$$\begin{cases} F_{\text{star}}(\alpha, t) = \sum_{v=1,9,11...}^{\infty} \dfrac{5N_{C1}I_{A1}}{v\pi} \cos(v\alpha - \omega t) \\[4mm] F_{\text{pentacle}}(\alpha, t) = \sum_{v=1,9,11...}^{\infty} \dfrac{5N_{C2}I_{A2}}{v\pi} \cos\left(v\left(\alpha - \dfrac{\pi}{10}\right) - \left(\omega t - \dfrac{\pi}{10}\right)\right) \end{cases} \tag{14}$$

F_{star} and F_{pentacle} represent the MMF of the star winding $A1$ and pentacle windings $A2$, respectively; and $N_{A1}(\alpha)$ and $N_{A2}(\alpha)$ represent the winding function of the windings $A1$ and $A2$, respectively.

The total air gap MMF distribution is given by

$$F_{\text{total}}(\alpha, t) = \begin{cases} \sum_{v=1,9,11...}^{\infty} \dfrac{10N_{C1}I_{A1}}{v\pi} \cos\dfrac{(v-1)\pi}{20} \cos\left(v\alpha - \omega t - \dfrac{v-1}{20}\pi\right), & v = 21, 41, ... \\[4mm] 0, & v \neq 19, 21, 39, 41... \\[4mm] \sum_{v=1,9,11...}^{\infty} \dfrac{10N_{C1}I_{A1}}{v\pi} \cos\dfrac{(v+1)\pi}{20} \cos\left(v\alpha + \omega t + \dfrac{v+1}{20}\pi\right), & v = 19, 39... \end{cases} \tag{15}$$

When $u = 1$ and $v = 19, 39$, harmonic magnetomotive force generated by the fundamental current is reverse rotating MMF with angular velocity $\omega/19$ and $\omega/39$, when $u = 1$, $v = 21, 41$, harmonic MMF generated by the fundamental current is a forward rotating MMF with angular velocity $\omega/21$ and $\omega/41$.

Furthermore, the angular velocity of the v-order harmonic MMF generated by a u-order harmonic current can be obtained by adopting the above method, as shown in Formula (12)

$$\omega_v = \begin{cases} -\dfrac{v\omega}{u}, & u + v = 20k, \ k = 0, \pm 1, \pm 2 \\[3mm] 0, & u + v \neq 20k, \ k = 0, \pm 1, \pm 2 \\[3mm] +\dfrac{v\omega}{u}, & u - v = 20k, \ k = 0, \pm 1, \pm 2 \end{cases} \tag{16}$$

where "+" indicates a forward rotating MMF, and "−" indicates a reverse rotating MMF.

3.3. MMF Characteristic Analysis

According to the analytic functions of the harmonic MMF of the two kinds of five-phase windings obtained in Sections 3.1 and 3.2, as well as the existing Y160L-4 three-phase motor, the MMF tables of three types of induction motors can be given. In the table, "+" indicates a forward rotating magnetomotive force, and "−" indicates a reverse rotating magnetomotive force. "F" indicates the phase advance, and "B" indicates the phase lag. Table 2 shows the MMF for the Y160L-4 type three-phase induction motor. Table 3 shows the MMF for the star winding five-phase induction motor. Table 4 shows the MMF for the pentacle-star winding five-phase induction motor.

Table 2. MMF for the Y160L-4 three-phase induction motor.

Time Harmonic	Spatial Harmonic					Total MMF
u	$v = 1$	$v = 5$	$v = 7$	$v = 11$	$v = 13$	$\sum$(MMF)
1	+1.053F	−0.211F	+0.150B	−0.096B	+0.081F	+0.977
5	−0.211B	+0.042B	−0.030F	+0.019F	−0.016B	−0.196
7	+0.150B	−0.030B	+0.021F	−0.014F	+0.012B	+0.139
11	−0.096B	+0.019F	−0.014B	+0.009B	−0.007F	−0.089
13	+0.081F	−0.016F	+0.012B	−0.007B	+0.006F	+0.076

Table 3. MMF for the star winding five-phase induction motor.

Time Harmonic	Spatial Harmonic					Total MMF
u	$v = 1$	$v = 3$	$v = 7$	$v = 9$	$v = 11$	$\sum$(MMF)
1	+1.156F	-	-	−0.128F	+0.105B	+1.133
3	-	+0.072B	−0.034B	-	-	+0.038
7	-	−0.034F	+0.014F	-	-	−0.02
9	−0.128B	-	-	+0.014B	−0.011F	−0.125
11	+0.105B	-	-	−0.011B	+0.009F	+0.103

Table 4. MMF for the pentacle-star winding five-phase induction motor.

Time Harmonic	Spatial Harmonic					Total MMF
u	$v = 1$	$v = 3$	$v = 7$	$v = 9$	$v = 11$	$\sum$(MMF)
1	+1.200F	-	-	-	-	+1.200
3	-	+0.1200B	-	-	-	+0.1200
7	-	-	+0.011B	-	-	+0.011
9	-	-	-	+0.002F	−0.002B	0
11	-	-	-	−0.002B	+0.002F	0

According to Tables 2–4, the following conclusions can be drawn:

1) When $u = v$, a synchronous MMF will come into being, which has the same synchronous speed as the fundamental MMF. The generated MMF can provide a linear superposition, reducing the peak value of magnetic density and air gap MMF, thus improving the waveform, utilization of iron core materials, and torque density.

2) When $u \neq v$, an asynchronous MMF will come into being, which generates torque pulsation, increases motor loss and noise, and reduces system performance.

3) When $u > 3$ for the three-phase winding, $u > 5$ for the star five-phase winding, or $u > 10$ for the pentacle-star five-phase winding, the amplitude and speed of the asynchronous MMF are larger than that of the synchronous MMF, which should be avoided as the asynchronous MMF will result in high torque pulsation and loss.

4) The lowest-order harmonic MMF generated by fundamental current differed, among which the lowest frequency of the three-phase winding was 5th-order; the lowest frequency of the star five-phase winding was 9th-order; and the lowest frequency of pentacle-star five-phase winding was 19th-order; further, the amplitude was far less than the MMF generated by fundamental current.

3.4. Performance Analysis of Electromagnetic Torque Using Synchronous MMF

According to the Ohm's Law of magnetic circuit, the relationship of magnetic field intensity, MMF, and magnetic permeability can be expressed as

$$H = f/L_s \tag{17}$$
$$B = kH \tag{18}$$
$$f = NI \tag{19}$$

Electromagnetic Force F can be expressed as

$$F = Bli = \frac{kfli}{L_s} = \frac{mkflI}{L_s} = \frac{mkf^2l}{NL_s} \tag{20}$$

Electromagnetic torque T_e can be expressed as

$$T_e = F\frac{D}{2} = \frac{mkf^2l}{NL_s}\frac{D}{2} \tag{21}$$

where H is the magnetic field intensity, f the MMF, L_s the length of stator closed flux linkage, k the magnetic permeability, I the current, D the inner diameter of stator, l the effective length of rotor winding, and m the current conversion factor.

When the permeability, stator inner diameter, and average length of the magnetic circuit are kept unchanged, the electromagnetic torque is proportional to the square of MMF.

According to the harmonic MMF analyses of the three different winding structures in Tables 2–4, it can be seen that the torque characteristics of the star winding five-phase motor can be improved by using the synchronous MMF generated by the 3rd-order harmonic, while that of the five-phase motor with pentacle-star winding can be improved by using the synchronous MMF generated by the 3rd-order and 7th-order harmonics.

Table 5 summarizes the results of the harmonic analysis. Although the synchronous velocity harmonic M.M.F was small, it allowed for a substantial increase in the output torque of the machine.

Table 5. Summary of harmonic MMF for three types of induction motor.

Motor Type	Winding Type	Amplitude and Useful Harmonic MMF				Performance Index
-	-	$v = 1$	$v = 3$	$v = 5$	$v = 7$	$\sum(\text{MMF})^2$
Three phase	Delta	+1.053	-	-	-	1.1088
Five phase	Star winding	+1.156	+0.072B	-	-	1.1203
Five phase	Pentacle winding	+1.20	+0.12B	-	+0.011B	1.4545

According to Table 5, the following conclusions can be drawn:

1) Without considering the use of harmonics, the electromagnetic torque of the five-phase motor with pentacle-star winding was better than that of the five-phase motor with star winding, as well as better than that of the traditional three-phase winding.

2) Under the condition of no harmonic injection, the existing harmonics can be considered to improve the electromagnetic torque, where the star winding five-phase motor's electromagnetic torque

was 21% higher than that of the three-phase winding, while that of the five-phase motor with pentacle-star winding was 31% higher than that of the three-phase winding.

3) If the injected 3rd-order harmonic is considered, the improvement of electromagnetic torque is more obvious. It was obvious that the pentacle-star winding five-phase motor had a more significant improvement, in terms of electromagnetic torque performance.

4. SIMULATION AND EXPERIMENTAL ANALYSIS

In order to further comprehend the performances of the two types of five-phase motors, the Finite Element Analysis (FEA) method was used.

The five-phase motor model with newly designed slot diagrams of stator and rotor was built based on Ansys Maxwell software, and the boundary conditions and excitation signals of the five-phase motor model are set to analyze its characteristics. Figure 6 shows the magnetic field density of star winding five-phase motor at different moments. Figure 7 shows the magnetic field density of pentacle-star winding five-phase motor at different moments. Figure 8 shows the air gap flux densities of two types of five-phase motors. Because of the adjustment of the winding connection mode, the magnetic field density is improved for the pentacle-star winding which can bring in better features.
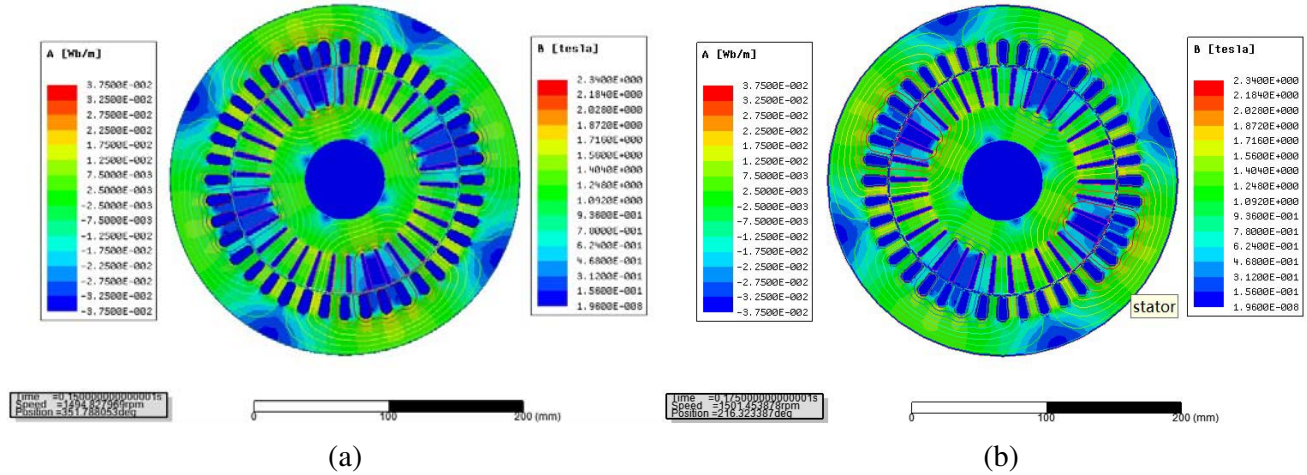

Figure 6. The magnetic field density of star winding five-phase motor, (a) when $t = 0.15$ s, (b) when $t = 0.175$ s.

A five-phase induction motor of two winding configurations was made based on a Y160L-4 three-phase induction motor with rated power 15 kW.

In order to analyse the performance of two types of five-phase motor, a prototype system was supplied by an inverter composed of two three-phase two-level voltage-source inverters sharing the same DC-link voltage, with each inverter phase leg operating independently. An STM32F407 high-performance microcontroller was used to control the inverter. A three-phase voltage regulator was used to adjust input voltage to obtain the different DC bus voltages shown in Table 1. Figure 9 is the prototype system.

The simple testing was carried out. Table 6 shows the main performance indexes of star and pentacle-star five-phase and Y160L-4 three-phase induction motors.

According to Table 6, the following conclusions can be drawn:

1) The designed two winding configuration five-phase motor saves on materials such as iron, copper, and aluminum, which can reduce manufacturing costs.

2) The rated efficiency of two types of five-phase motor is higher than three-phase motor, which means increased energy efficiency.

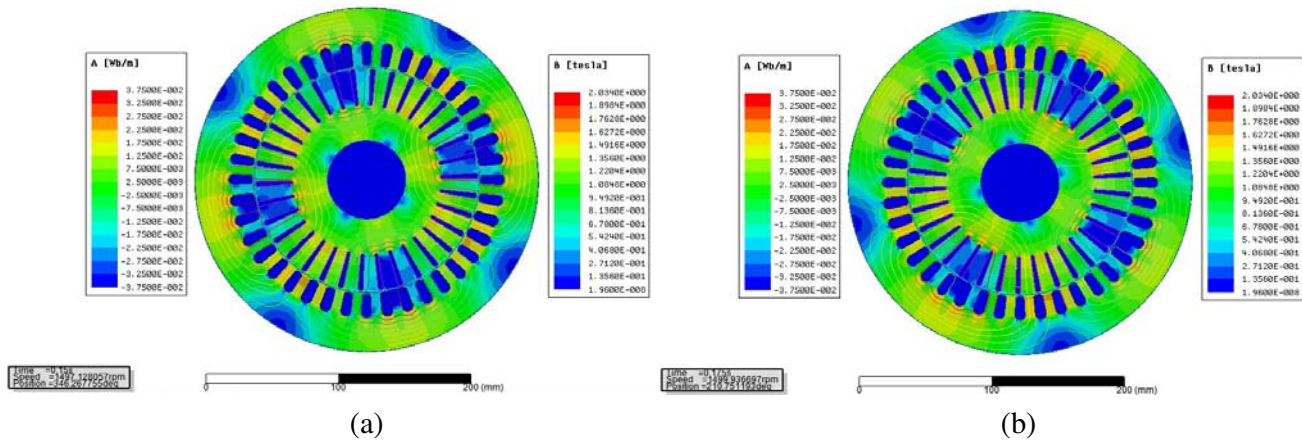3) The rated power factor for pentacle-star winding five-phase motor is the best.

(a) (b)

Figure 7. The magnetic field density of pentacle-star winding five-phase motor, (a) when $t = 0.15$ s, (b) when $t = 0.175$ s.
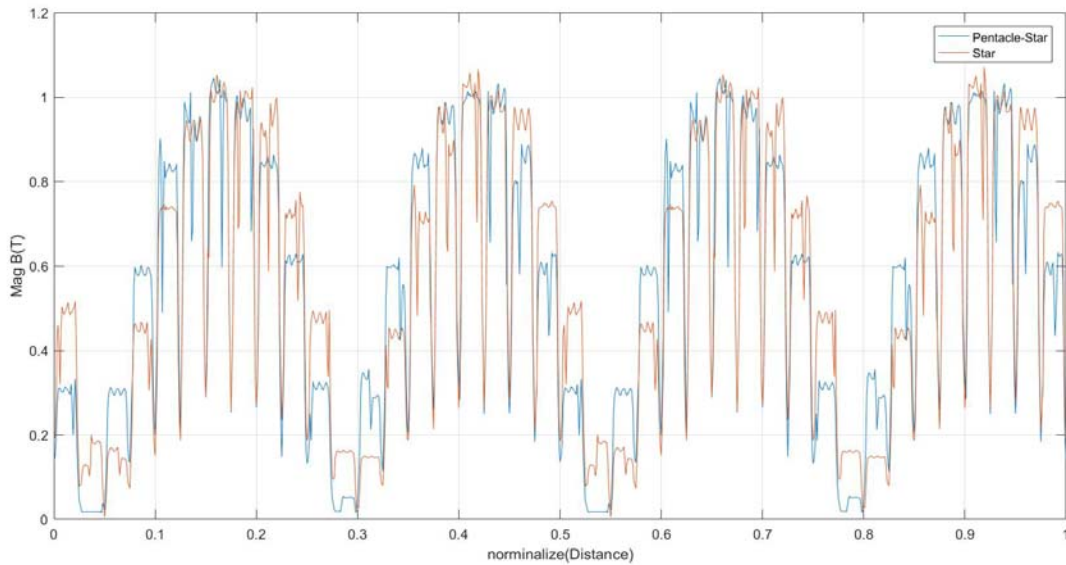

Figure 8. Air gap flux density for five-phase motor: star winding and pentacle-star winding.

Table 6. Performance indexes for three types of induction motor with the same rated power.

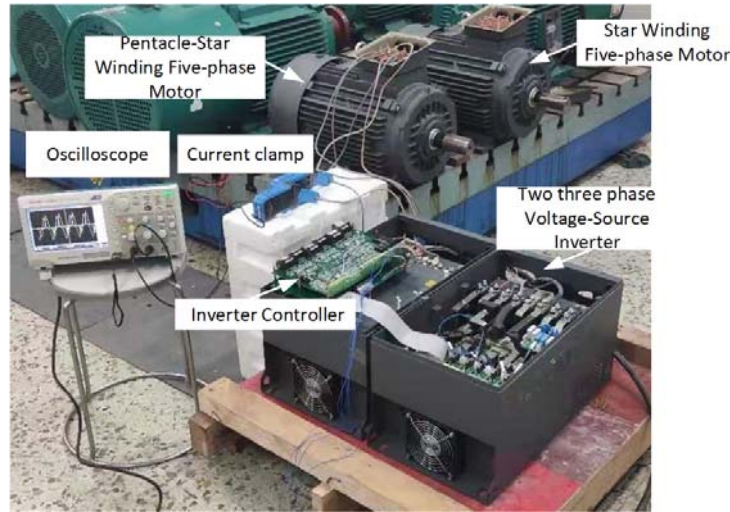| Phase Number	3	5	5
Winding Configuration	Delta connection	Star connection	Pentacle-Star connection
Iron Weight (kg)	97.7	95.2	95.2
Sator Cu Weight (kg)	9.98	9.42	9.42
Rotor Al Weight (kg)	1.82	1.62	1.62
Ratio peak torque multiple	2.418	2.263	2.525
Rated efficiency (%)	89.72	90.31	90.73
Rated power factor	0.856	0.851	0.862
Rated slip	0.025	0.026	0.026

Figure 9. Pentacle-star and star five-phase prototype motor based on Y160L-4.

5. CONCLUSIONS

Through the research in this paper, the following beneficial results were obtained:

1) Based on a Y160L-4 15 kW three-phase motor, keeping the main structural parameters constant, two types of five-phase motor can be implemented (using star winding or pentacle-star winding), only requiring reconstruction of the stator winding, adjustment of the slot numbers for the stator and rotor, and redesigning of the stator and rotor trough. This method is fast, efficient, and has low cost with high engineering application value.

2) Based on Fourier series expansion and analytical methods, the harmonic MMFs under non-sinusoidal power supply were given for the star and pentacle-star windings. The two proposed types of five-phase motor had better properties than the three-phase motor. For the star and pentacle-star winding five-phase motors, the lowest harmonic MMFs produced by the fundamental wave current were 9th-order and 19th-order, respectively, which reduce the effect of motor performance.

3) For the same power driving conditions, considering electromagnetic torque generated by the harmonic MMF, the five-phase motors using pentacle-star and star windings had electromagnetic torque increases, compared with a traditional three-phase motor.

4) Further, according to the three kinds of winding connection-pentacle-star, star, and delta, pentacle-star winding has the best tolerance. Future work such as phase absence and torque characteristic will assess the performance of the three motor types through further experimental research.

REFERENCES

1. Yaday, K. B., A. K. Mohanty, and P. Kumar, "Recent research trend on multi-phase induction machines," *Conf. on Control, Communication and Power Engineering*, 580–586, 2014.

2. Levi, E., R. Bojoi, F. Profumo, H. A. Toliyat, and S. Williamson, "Multiphase induction motor drives — A technology status review," *IET Electr. Power Appl.*, Vol. 1, No. 4, 489–516, 2007.

3. Pellegrino, G., A. Vagati, B. Boazzo, and P. Guglielmi, "Comparison of induction and PM synchronous motor drives for EV application including design examples," *IEEE Transaction on Industry Applications*, Vol. 48, No. 10, 2322–2332, 2012.

4. Nguyen, N. K., E. Semail, F. Meinguet, and P. Sandulescu, "Different virtual stator winding configurations of open-end winding five-phase PM machines for wide speed range without flux weakening operation," *EPE 2013*, Vol. 34, No. 10, 1064–1076, 2013.

5. Klingshirn, E. A., "High phase order induction motors — Part II: Experimental results," *IEEE Transaction on Power Apparatus and System*, Vol. PAS102, 54–59, 1983.

6. Singh, G. K., "Multi-phase induction machine drive research — A survey," *Electr. Power Syst. Res.*, Vol. 61, 139–147, 2002.

7. Ward, E. E. and H. Harer, "Preliminary investigation of an inverter fed 5-phase induction motor," *Electrical Engineers, Proceedings of the Institution*, Vol. 116, No. 5, 980–984, 1969.

8. Levi, E., "Multiphase electric machines for variable-speed applications," *IEEE Transaction on Industrial Electronics*, Vol. 55, No. 5, 1893–1909, 2008.

9. Sawahata, M., K. Nishihama, and H. Nikami, "Magnetic flux density analysis of wound rotor induction motor by permeance model," *ICEMS 2009*, Vol. 34, No. 10, 1064–1076, 2009.

10. Schreier, L., J. Bendl, and M. Chomat, "Analysis of fault tolerance of five-phase induction machine with various configurations of stator winding," *EDPE 2015*, 196–203, 2015.

11. Liang, X. and Y. Luy, "Harmonic analysis for induction motors," *IEEE CCECE/CCGEI*, Vol. 34, No. 10, 1064–1076, 2006.

12. Kindl, V., R. Cermak, Z. Ferkova, and B. Skala, "Review of time and space harmonics in multi-phase induction machine," *Energies*, Vol. 13, 496, 2020.

13. Wu, X., D. Wang, Y. Guo, et al., "Effect of stator winding combination modes for multiphase electric machines on MMFS and parameters," *CSEE*, Vol. 34, No. 10, 2944–2951, 2014.

14. Kocabas, D. A., "Novel winding and core design for maximum reduction of harmonic magnetomotive force in AC motors," *IEEE Transactions on Magnetics*, Vol. 45, No. 2, 735–746, 2009.

15. Kowal, A., M. R. Arahal, C. Martin, and F. Barrero, "Constraint satisfaction in current control of a five-phase drive with locally tuned predictive controllers," *Energies*, Vol. 12, 2715, 2019.

16. Abdel-Khalik, A. S. S., S. Ahmed, and A. M. Massoud, "Low space harmonics cancelation in double-layer fractional slot winding using dual multiphase winding," *IEEE Transactions on Magnetics*, Vol. 51, No. 5, 8104710, 2015.

17. Lei, Y., Z. Zhao, and D. G. Dorrell, "Design and analysis of star-delta hybrid windings for high-voltage induction motors," *IEEE Transactions on Industrial Electronics*, Vol. 58, No. 9, 3758–3767, 2011.

18. Sadeghi, S., L. Guo, and H. A. Toliyat, "Wide operational speed range of five-phase permanent magnet machines by using different stator winding configurations," *IEEE Transactions on Industrial Electronics*, Vol. 59, No. 6, 2621–2631, 2012.

19. Masoud, M. I., "Five phase induction motor: Phase transposition effect with different stator winding connections," *IECON 2016*, 1648–1655, 2016.

20. Abdel-Khalik, A. S., et al., "Steady-state mathematical modeling of a five-phase induction machine with a combined star/pentagon stator winding connection," *IEEE Transactions on Industrial Electronics*, Vol. 63, No. 3, 1331–1343, 2016.

21. Abdel-Khalik, A. S., et al., "An improved fault-tolerant five-phase induction machine using a combined star/pentagon single layer stator winding connection," *IEEE Transactions on Industrial Electronics*, Vol. 63, No. 1, 618–628, 2016.

22. Mohammadpour, A., S. Sadeghi, and L. Parsa, "A generalized fault-tolerant control strategy for five-phase pm motor drives considering star, pentagon, and pentacle connections of stator windings," *IEEE Transactions on Industrial Electronics*, Vol. 61, No. 10, 63–75, 2014.

23. Xu, S., *Winding Theory of AC Motor*, China Machine Press, Beijing, 1985.

24. Edelson, J. S., "High phase order motor with mesh connected windings," U.S. Patent 6 831 430, Dec. 14, 2004.

25. Buening, D., "Five phase alternating current generator," Eur. Patent EP1 29 643 9A2, Mar. 26, 2003.

26. Abdel-Khlik, A. S., A. S. Morsy, S. Ahmed, and A. M. Massoud, "Effect of stator winding connection on performance of five-phase induction machines," *IEEE Transactions on Industrial Electronics*, Vol. 61, No. 1, 3–19, 2014.

27. Gao, H., G. Yang, J. Liu, and P. Zhao, "Air-gap MMF analysis for five-phase PMSM with third harmonic injection," *Electronic Machines and Control*, Vol. 17, No. 10, 1–6, 2013.

28. Zhao, B. and G. Li, "The analysis of multiphase symmetrical motor winding MMF," *Electronic Engineering and Automation*, Vol. 2, No. 2, 11–18, 2013.

29. Rangari, S. C., H. M. Suryawanshi, and B. Shah, "Harmonic content testing for different connections of five-phase induction motor," *ICPS2016*, 2016.

30. Sadeghi, S., L. Parsa, and H. A. Toliyat, "Extending speed range of five-phase PM machines by changing the stator windings connections," *IEMDC*, 1540–1545, 2011.